Magnetism of 3d-Transition Metal (Fe, Co, and Ni) Nanowires on w-BN (0001)

ARTICLE *in* THE JOURNAL OF PHYSICAL CHEMISTRY C · AUGUST 2009

Impact Factor: 4.77 · DOI: 10.1021/jp810124k

3 AUTHORS, INCLUDING:

Guang-Yu Guo
National Taiwan University
258 PUBLICATIONS **4,692** CITATIONS

SEE PROFILE

Magnetism of 3d-Transition Metal (Fe, Co, and Ni) Nanowires on w-BN (0001)

S. J. Luo,*,†,‡ G. Y. Guo,† and A. Laref†

Department of Physics, National Taiwan University, Taipei 106, Taiwan, and Department of Basic Sciences, Hubei Automotive Industries Institute, Hubei 442002, China

Received: November 18, 2008; Revised Manuscript Received: February 24, 2009

We study the magnetic properties of monoatomic Fe, Co, and Ni nanowires on wurtzite boron nitride (w-BN)(0001) using state-of-the-art first-principles calculations. Our results show that the most stable phase is the ferromagnetic Co(Fe) metal-atom chain adsorbed on the w-BN(0001) surface terminated by N layers. The monoatomic Co and Ni chains on the w-BN (0001) surface terminated by N layers are found to be excellent half-metallic ferromagnets with large half-metallic gaps (up to 0.65 eV). The monoatomic Co and Fe nanowires on B-terminated w-BN (0001) and Fe nanowires on N-terminated w-BN (0001) present large but not complete spin polarization. We found that the large magnetic anisotropy energy (MAE) of ferromagnetic atoms is caused by a magnetic Coulomb interaction between the ferromagnetic atoms and N and B atoms. In this case, the large spin−orbit coupling of the ferromagnetic atoms and the hybridization between the ferromagnetic atoms d-, N p-, and B p-like states are crucial. The w-BN (0001) surface acts as a simple structural template with the transition metal (TM) (Fe, Co, and Ni) chains for the formation of an artificial one-dimensional system. We demonstrate that the magnetic properties of TM atomic chains on the w-BN(0001) surface are responsible for different couplings with the substrate which are significant for future experiment investigations.

I. Introduction

During the last few decades, numerous studies related to the novel magnetic phenomena of magnetic materials in reduced dimensions have been undertaken.[1,2] Ferromagnetic metal nanostructures on flat and stepped W(110) surfaces have been extensively studied.[3−7] A prominent example is iron films on W(110) which can be prepared in the form of stable pseudomorphic monolayers (ML) for a wide temperature range[8,9] and thus are ideally suited for investigation of genuine two-dimensional magnetic phase transitions.[10] The combination of conversion-electron Mössbauer spectroscopy (CEMS) to measure the temperature-dependent magnetic hyperfine fields, with torsion oscillation magnetometry which provides the absolute size of magnetic moments, has made it possible to determine the magnetic moment in a Fe/W(110) adlayer, $S = 2.53 \pm 0.12\mu_B$ (ref 3). This value represents an extrapolation to zero temperature, and can therefore be directly compared with theoretical estimates stemming from self-consistent local-spin-density calculations $S = 2.18\mu_B$ (ref 4), $S = 2.54\mu_B$ (ref 5), and $S = 2.12\mu_B$ (ref 6). Gambardella et al. experimentally investigated the magnetism of single Co atoms and Co nanoparticles on a Pt(111) surface.[11] They found that the spin magnetic moment is very stable and nearly independent of the coordination. In contrast, the orbital magnetic moment decreases strongly with increasing Co coordination, from 1.10 μ_B/atom for the single Co atom to 0.22 μ_B/atom for the tetramer. The MAE also decreases strongly with increasing Co coordination. A giant MAE of 9 meV/atom for single Co atoms was found, which is assumed to arise from the combination of unquenched orbital moments (1.1 Bohr magnetons) and strong spin-orbital coupling induced by the platinum substrate. Very lately, Shick et al.[12] studied theoretically the magnetism of single Co atoms on Pt(111) surface using LSDA+U method. The authors pointed out that two major effects should be included in order to improve the Co orbital magnetic moment: (i) structural relaxation of the Co−Pt interatomic distance and (ii) the orbital polarization in LSDA. According to the recent experimental work,[13] it is not certain that the metallic wires will order ferromagnetically. In fact, the authors claim that the ideal infinite chain of atoms cannot sustain ferromagnetic order at nonzero temperature, whereas the Curie temperature is only of the order of 10 K for Co wires on a Pt surface. Gambardella et al.[13] have shown that the stability of the ferromagnetism in monoatomic cobalt chains at finite temperatures could be controlled by the finite length of the chains and magnetic anisotropy barriers. In this respect, the ferromagnetism in 3d TM chains on insulator substrates may not persist at finite temperatures. So, it would be of great interest to explore experimentally the magnetism in 3d TM chains deposited on the BN surface at finite temperatures.

Recently, Gambardella et al. succeeded in observing ferromagnetism of monoatomic Co wires decorating the Pt(997) surface step edge. By exploiting the element-selectivity of the X-ray magnetic circular dichroism (XMCD), the existence of long-range-like ferromagnetic order on Co was demonstrated below 15 K.[13,14] Although theoretically the Mermin−Wagner theorem[15] forbids long-range 1D ferromagnetic order at nonzero temperatures, ferromagnetism in 1D can be stabilized by a large MAE, which creates barriers effectively blocking thermal fluctuations. The significance of such a blocking mechanism was recognized earlier for the occurrence of long-range magnetic order in 2D systems.[16,17]

The experiments of Gambardella et al. revealed novel magnetic properties of monoatomic Co wires at Pt step edges. An unexpected magnetocrystalline anisotropy was observed where the easy magnetization axis was directed along a peculiar angle of + 43° toward the Pt step edge and normal to the Co

* To whom correspondence should be addressed.
† National Taiwan University.
‡ Hubei Automotive Industries Institute.

10.1021/jp810124k CCC: $40.75
Published on Web 07/22/2009

chain. The MAE was estimated to be substantial, of the order of 2 meV/Co atom.[13] In addition, a considerable enhancement of the Co orbital magnetic moment $L \sim 0.7\mu_B$ relative to the bulk Co L value of $0.14\mu_B$ was deduced from XMCD experiments.

Half-metallic ferromagnets are seen as a key ingredient in future high performance spintronic devices because they have only one electronic spin channel at the Fermi energy and therefore may show nearly 100% spin polarization.[18,19] Since de Groot et al.'s discovery[20] in 1983, many half-metallic ferromagnets have been theoretically predicted, and furthermore, some have also been confirmed experimentally.[21−24] Much attention has been devoted to understanding the mechanism behind the half-metallic ferromagnetism and studying its implications on various physical properties.[25] The nanostructural half-metallic ferromagnets have many potential applications in spintronic devices due to their peculiar properties. For this purpose, we devote ourselves to the search for nanostructural half-metallic ferromagnets. We show that the ferromagnetic TM monoatomic wires on insulator substrates may be very promising candidates. Another reason for this work is that ferromagnetic metal nanostructures on metal substrates have previously demonstrated fascinating phenomena. To our knowledge, the magnetism of ferromagnetic metal nanostructures on insulator substrates has not been reported as yet. The w-BN has outstanding physical and chemical properties such as extreme hardness, very high thermal conductivity and melting temperature, wide band gap and low dielectric constant. These advantageous features make it desirable for many applications in modern microelectronic devices.[26,27] These attributes assist in the growth of flat films or wires free from any noticeable intermixing, proving that the dense and stable w-BN (0001) surface is an excellent substrate.

In order to search for nanostructural half-metallic ferromagnets, we systematically explore the monoatomic Fe, Co and Ni nanowires on the w-BN (0001) surface terminated by both N and B layers, respectively. However, particular attention is devoted to the influence of reduced dimensionality and adsorbate−substrate hybridization on the magnetic properties of Fe, Co, and Ni nanostructures. We present a comprehensive study of the magnetic and electronic properties of atomic chains (Fe, Co, and Ni) adsorbed on the w-BN(0001) surface. We will discuss the interplay between the nature of the atomic chains and the ferromagnetic behavior that arises from different levels of interaction with the substrate. In this paper, we report a theoretical investigation on the phase stability, electronic structure, magnetic moment, and the MAE of monoatomic Fe, Co, and Ni nanowires on the w-BN (0001) terminated by N and B layers using DFT calculations.[28]

II. Computational Details

Our theoretical calculations are performed using the Vienna ab initio simulation package (VASP).[29−31] We describe the interaction between ions and electrons using the frozen-core projector augmented wave (PAW) approach. The overall framework is spin-polarized density-functional theory (DFT) in the generalized-gradient approximation (GGA). Our GGA calculation for bulk w-BN gives lattice parameters $a = 2.557$ Å and $c = 4.230$ Å, which are in good agreement with the experimental lattice constants $a = 2.532$ Å and $c = 4.188$ Å.[32] The infinite surface was simulated by a large supercell corresponding to 1×2 surface cell. We have also included a thick layer in the directions perpendicular to the surface to prevent spurious interactions between adjacent replicas. For the study

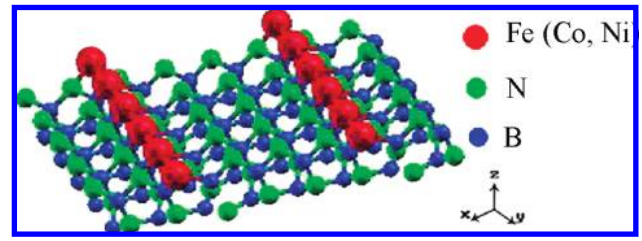

Figure 1. Schematic nanostructure used to represent the Fe, Co and Ni nanowires on the w-BN (0001). The red ball, green ball, and blue ball are Fe (Co and Ni), N, and B, respectively.

of monoatomic Fe, Co, and Ni nanowires on the w-BN (0001) surface terminated by B and N layers respectively, the real system is simulated by a slab consisting of seventeen N and B atom layers (eight B and N atom layers on each side of the center layer symmetrically). The system also includes the monoatomic TM (Fe, Co, and Ni) nanowires on each side of the w-BN slab and a 14 Å thickness vacuum space (Figure 1). The atomic positions were relaxed by minimizing the forces according to a quasi-Newton algorithm.[33] During relaxation, the middle thirteen layers were kept fixed at bulk positions and in the rest only the vertical positions were optimized. For all cases, the two B and N top layers including the chain atoms were relaxed out of plane until forces on the atoms were lower than 0.0001 eV/Å. We used $20 \times 20 \times 1$ k-points within the two-dimensional irreducible Brillouin zone (BZ) in order to calculate the total energy and MAE of different magnetic states. We note that all energy differences in this paper are understood to be per Fe (Co and Ni) atom. The cutoff energy is taken to be 500 eV, and the convergence criterion for energy is 10^{-5} eV.

III. Results and Discussion

A. Adsorption Energies of Monoatomic TM = (Fe, Co, and Ni) Nanowires on w-BN(0001) Surface. First we present the structural stability results for the ferromagnetic monoatomic TM chains along the [0001] direction, which are simulated by adding TM atoms to the bridge of N surface, troughs the (1×2) unit cell. We choose typical ferromagnetic metals Fe, Co, and Ni as the adsorbed materials and w-BN is chosen as the substrate. We have performed a structure optimization of the Fe, Co and Ni nanowires on the w-BN (0001) surface terminated by N layers. The detailed atomic structure of the best-fit structure of the Fe, Co and Ni nanowires on the w-BN (0001) surface terminated by N layers, are given in Table 1. The distances between the Fe (Co, Ni) nanowires and the first layer, the first layer and the second layer, the second layer and third layer are denoted by d_{01}, d_{12}, and d_{23}, respectively. The distance d_{12} for all three nanostructures is contracted in comparison with the corresponding bulk interlayer spacing, but in contrast, the distance d_{23} is expanded. In Table 2, we compare the adsorption energy (E_{Ads}) of the ferromagnetic atomic chain on the surface and the formation energy of a ferromagnetic isolated chain (E_{Chain}) with the same geometry. E_{Ads} is the energy difference between the surface with and without adsorbate:

$$E_{Ads} = E_{Tot}^{TM/BN} - E_{Tot}^{BN} - E_{Tot}^{Chain} \quad (1)$$

while E_{Form}^{Chain} is the energy difference between the isolated chain and the single atom

$$E_{Form}^{Chain} = E_{Tot}^{Chain} - E_{Tot}^{atom} \quad (2)$$

TABLE 1: Theoretically Predicted Structure[a]

interlayer relaxation (Å)	Fe on B-s	Co on B-s	Ni on B-s
d_{01}	1.914	1.803	1.932
d_{12}	0.693	0.671	0.672
d_{13}	1.815	1.814	1.815

[a] d_{01}, d_{12}, and d_{23} are defined as the distances between the Fe (Co, Ni) nanowires and the first N layer, the first layer and the second layer, and the second layer and third layer, respectively.

TABLE 2: Adsorption Energies of Chains Ad (Fe, Co, and Ni) on w-BN(0001) Surface, Including the Formation Energies of the Isolated Chain[a]

E_{Ads} (relaxed)			E_{Form} (chain)		
Fe	Co	Ni	Fe	Co	Ni
−1.016	−0.953	−0.596	−0.273	−0.224	−0.165

[a] All quantities are calculated in eV.

TABLE 3: Structural Parameters for Relaxed w-BN(0001) Surface Ad/BN(0001)-(1 × 2)[a]

	d(B−N)		ω		
	in plane	lateral	in plane	lateral	Δz(Ad−N)
clean	1.543	1.556	34.992	34.953	
Fe chain	1.595	1.484	35.536	35.773	2.136
Co chain	1.617	1.511	35.814	35.974	2.157
Ni chain	1.626	1.528	35.405	35.643	2.184

[a] Distances are expressed in Å and angles in deg. d(B−N) is the atomic B−N distance, ω is the in-plane B−N angle along the [0100] direction, and Δz is the vertical B−N interlayer spacing.

where E_{Tot}^{Chain} is the total energy of an isolated chain calculated in the same unit cell, and E_{Tot}^{atom} is the total energy of the atom. From Table 2, it is clear that the formation of the chain is energetically favorable in the case of Fe (Co) TM adsorbed on the BN surface. However, the relaxed Fe (Co) wires are thermodynamically stable. This is due to the attractive interaction between the chains and the substrate. We find that a stable Fe (Co) chain only forms when it is in the bridge of N atoms. The TMs (Fe, Co, and Ni) present a characteristic trend going from Fe to Ni shown in table 2. As the d shell is filled, the adsorption energy (E_{Ads}) increases correspondingly with an increase in the vertical distance [Δz(Ad−N)] (see Tables 2−3). This fact suggests that the filling of the valence d shell reduces the coupling with the substrate. The Fe−Fe distance (2.491 Å) is induced by the N−N periodicity. The interatomic separation is larger than the equilibrium distance in isolated chains. Indeed, if we relax the Fe−Fe distance in chains without the substrate the bond length shrinks down to 2.283 Å. This geometry would have a formation energy of −0.273 eV/atom, greater than that with the presence of the substrate (Table 2). Despite the energetic gain in the formation of the chain/surface interface, the overall distortions of the substrate induced by the atomic chains are small. Table 3 displays the structural parameters (bond length and angles) for the w-BN (0001) surface terminated by N layers. The ideal cleavage surface undergoes a structural relaxation, which primarily involves the atoms in the first two N layers, on the top layer of the BN(0001) surface, as summarized in Table 3. In the optimized structure, we observe a vertical displacement Δz of N atoms with a small distortion in plane. The structural modifications are negligible for all other planes except the top two B and N layers respectively including the atomic chains. Hereafter we will refer only to the relaxation of the first N layer out of plane including the atomic chains.

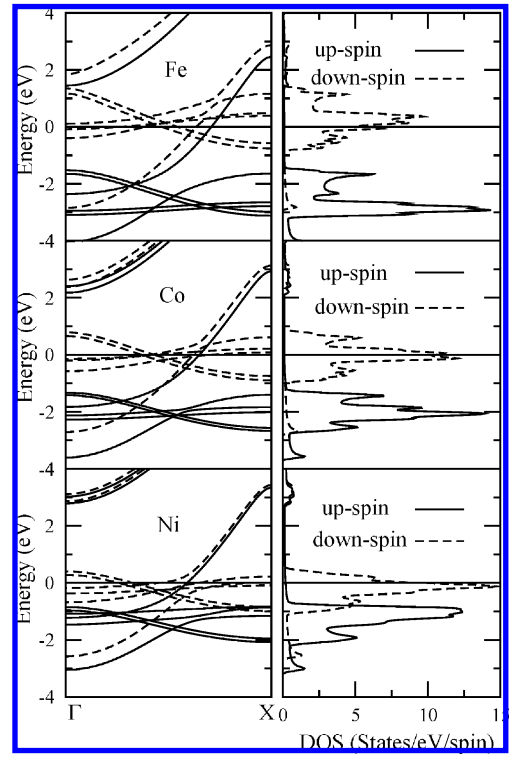

Figure 2. GGA density of states of the isolated Fe, Co and Ni chains. The solid (dashed) line denotes the up (down) spin. The Fermi level is set at zero.

We explicitly separate the results regarding the atoms that are nearest-neighbor to the chains, from those in the adjacent unit cell (labeled "Lateral"). The atomic reorganization of the substrate is more appreciable in the unit cell containing the chain atoms. The small distortion of the surface close to the adsorption site and its rapid decay along the [0001] direction is the first signature of the one-dimensional (1D) nature of Co (Fe) chains. Our results could be easily supported by experimental study.

B. Isolated Fe, Co, and Ni Chains in a Vacuum. We now discuss the results of the electronic structure and magnetism for the isolated Fe, Co, and Ni chains in a vacuum. We use the same geometric configuration as the ferromagnetic metal Fe (Co, Ni) nanowires adsorbed on the w-BN (0001). In the present calculations the relaxed atomic distances of Fe, Co, and Ni chains are 2.283, 2.311, and 2.344 Å, respectively, where the chains are along the y axis. Figure 2 displays the band structure and the density of states (DOS) of the isolated Fe, Co, and Ni chains in the vacuum. From Figure 2, we find that the up-spin orbitals of the ferromagnetic atoms Fe, Co, and Ni are almost fully filled, and the up-spin DOS of the Co and Ni shift toward higher energy compared with that of the isolated Fe. In contrast, the down-spin DOS of the Co and Ni shift toward lower energy compared with that of the isolated Fe. This is due to their isostructure and their number of 3d valence electrons increasing from Fe to Co to Ni. In fact, the number of d-electrons determines the position of these states with respect to Fermi energy. In order to avoid confusion, we must point out that the up-spin DOS in Figure 2 are of the order of 10^{-1} in the vicinity of the Fermi level. The spin magnetic moments are 3.188μ_B/Fe, 2.217μ_B/Co, and 1.168μ_B/Ni, respectively. It is interesting to note that the spin magnetic moment differences between Fe and Co and Co and Ni are about 1.0μ_B, which is almost the same as the difference among their valence electrons. The extra one 3d electron of Co and the extra two 3d electrons of Ni in contrast to the valence electrons of Fe, occupy down-spin 3d

TABLE 4: GGA Calculated Spin Moments S (μ_B), Orbital Moments L (μ_B), and MAE (meV) Per Ferromagnetic Metal Atom for the Isolated Fe, Co, and Ni Chains

metal	S	L	ΔL_{x-z}	ΔE
Fe	3.188	0.237	−0.104	0.576
Co	2.217	0.238	−0.072	0.297
Ni	1.168	0.497	−0.366	7.56

TABLE 5: Calculated Total Energies E of the Supercell for Ferromagnetic (FM), Antiferromagnetic (AF), and Nonmagnetic (NM) States Relative to the Ground State for the Fe, Co, and Ni Nanowires on the w-BN (0001) Surface Terminated by B Layers

	Fe	Co	Ni
E_{FM} (meV)	0	0	0
E_{AF} (meV)	41.50	137.11	22.29
E_{NM} (meV)	528.77	241.26	91.37

orbitals. This is very likely due to the fact that the up-spin 3d orbitals are almost fullyfilled in the case of Fe (Co, Ni) isolated chain (see the figures of the band structures and DOS of Fe, Co and Ni). In addition, a considerable enhancement of the spin magnetic moments relative to Fe, in Co and Ni bulk values was induced by the dimensionality reduction effect (1D), leading to a more atomic-like configuration.

The calculated spin and orbital magnetic moments in μ_B and MAE per ferromagnetic metal atom are compiled in Table 4. We define $\Delta L_{x-z} = L_x - L_z$, where L_x and L_z are the orbital moments for the magnetization direction fixed along the x and z axis respectively, the MAE $\Delta E = E^{100} - E^{001}$, where E^{100} and E^{001} are the total energies with the magnetization in the [100] and [001] direction, respectively. Table 4 shows that the MAE increases strongly with increasing absolute value of the orbital moments difference ΔL_{x-z}. It is worth mentioning that the MAE is the energy required to rotate the magnetization from its ground state direction called the easy direction to the hardest direction. This rotation influences the magnetic properties of low-dimensional magnetic nanostructures or the atomic chains.

C. Fe, Co, and Ni Nanowires on the w-BN(0001) Surface Terminated by B Layers. We study the magnetic properties of Fe, Co, and Ni nanowires adsorbed on the w-BN (0001) terminated by B layers in this part. We use, as a unit cell, the 1×2 supercell doubled along the b direction to calculate the total energy for different magnetic states. Three magnetic configurations: a ferromagnetic, a nonmagnetic and an antiferromagnetic configuration were considered. In the antiferromagnetic calculations, we assume an antiparallel alignment of the spin of the atoms in the two unit cells in the b direction. The calculated relative total energies E for different magnetic states with respect to the ferromagnetic state are summarized in Table 5. We find that the ferromagnetic state is a ground state for all three nanostructures. The interactions among Fe (Co, Ni), B, and N are obviously of crucial importance in these three particular systems, since in a free-standing Fe (Co, Ni) chain these three kinds of ferromagnetic metal atoms have much bigger spin moments than that of the ferromagnetic metal atoms adsorbed onto the B surface of the w-BN(0001) (see Table 4 and Table 6). Figure 3 shows the calculated atom-resolved DOS of the Fe, Co and Ni nanowires on the B-terminated w-BN (0001). In comparison with the DOS of the isolated Fe(Co, Ni) chain, we notice that when the Fe (Co, Ni) chains are brought into contact with the B-terminated w-BN (0001), the hybridization between the Fe (Co, Ni) d- and B p-like orbits leads to a mutual attraction of the Fe (Co, Ni) 3d, B 2p and N 2p bands. Both the up-spin and down-spin bands of the Fe (Co, Ni) atoms

TABLE 6: GGA Calculated Spin Magnetic Moments in μ_B for the Fe, Co, and Ni Nanowires on the w-BN (0001) Surface Terminated by B Layers[a]

	Fe (Co, Ni)	first ly B1	first ly B2	second ly N1	second ly N2	third ly B1	third ly B2
Fe	2.286	0.278	–0.112	–0.023	0.03	0.02	0.00
Co	0.924	0.272	–0.063	–0.024	0.03	0.02	0.00
Ni	0.368	0.276	0.011	–0.022	0.01	0.01	0.00

[a] In the table, the B1 of the first layer denotes the B atom which is second furtherest away from the nanowire, and the B2 is the nearest neighbor B atom of the nanowires in the first layer. We adopt the same rule to label atoms in other layers. The word layer is abbreviated to ly in this table and figures.

are pushed toward the Fermi level. The B 2p and N 2p bands are also attracted to the Fermi level in comparison to those of B and N in the bulk BN (Figure 5). The spin moments of the ferromagnetic metal atoms Fe (Co, Ni) adsorbed onto the B surface of the w-BN (0001) decrease almost by $1.0\mu_B$ compared with that in the free-standing chains. It is worth mentioning that the induced magnetic moments on the B and N atoms are very similar for all three nanostructures (see Table 6). In the vicinity of the Fermi level, the DOS of the neighboring B and N atoms between the adjacent layers are almost the same. However, this can be explained by the strong covalent coupling among them. The shapes of the DOS in the top three layers of the substrates supporting the Fe (Co, Ni) nanowires are similar. The DOS spectra of the third layer and below is similar to that of the innermost (fifth and sixth) layer (as displayed in Figure 5). The DOS of the innermost layers in other cases are similar to that shown in Figure 5, and resemble that of B and N of the bulk w-BN. The spin polarization is defined as $[N_\downarrow(E_F) - N_\uparrow(E_F)]/[N_\downarrow(E_F) + N_\uparrow(E_F)]$, where $N_\uparrow(E_F)$ ($N_\downarrow(E_F)$) represents the DOS of the up- (down-) spin at the Fermi level. The layer- and spin-decomposed DOS spectra of the Fe and Co nanowires on the B-terminated w-BN (0001) near the Fermi level are highly polarized due to the presence of the ferromagnetic nanowires. The DOS of Ni in the Ni nanowires on the B-terminated w-BN (0001) surface is significantly different from that in the isolated Ni chain. However, there is no spin splitting at all. On the other hand, the B and N atoms exhibit nearly the same electronic and magnetic properties as in the case of Fe and Co nanowires on B-terminated w-BN (0001) surface.

D. Fe, Co, and Ni Nanowires on the w-BN(0001) Surface Terminated by N Layers. We turn now to the discussion of the magnetic properties of Fe, Co and Ni nanowires on the w-BN(0001) surface terminated by N layers. The calculated magnetic energy differences of the three nanostructures in different magnetic states are presented in the Table 7. It is evident that all these nanostructures prefer a ferromagnetic configuration. Figure 4 illustrates the calculated atom-resolved DOS of the Fe, Co, and Ni nanowires on the N-terminated w-BN (0001). In the plotted energy range, from −8 to +6 eV, the total DOS of Fe (Co, Ni) is mainly attributed to d-like orbitals, and the total DOS of N (B) is mainly originated from p-like orbitals. For simplicity, we do not additionally give the partial DOS of these atoms.

The large induced magnetic moments on N and B atoms are principally from the strong hybridizations between Fe (Co, Ni) d- and N p-like orbitals. The spin moments induced on the N and B atoms decrease rapidly from the top layer to the center layer. Table 8 gives the calculated spin moments of the various atoms for the Fe (Co, Ni) nanowires on the N surface of the w-BN (0001).

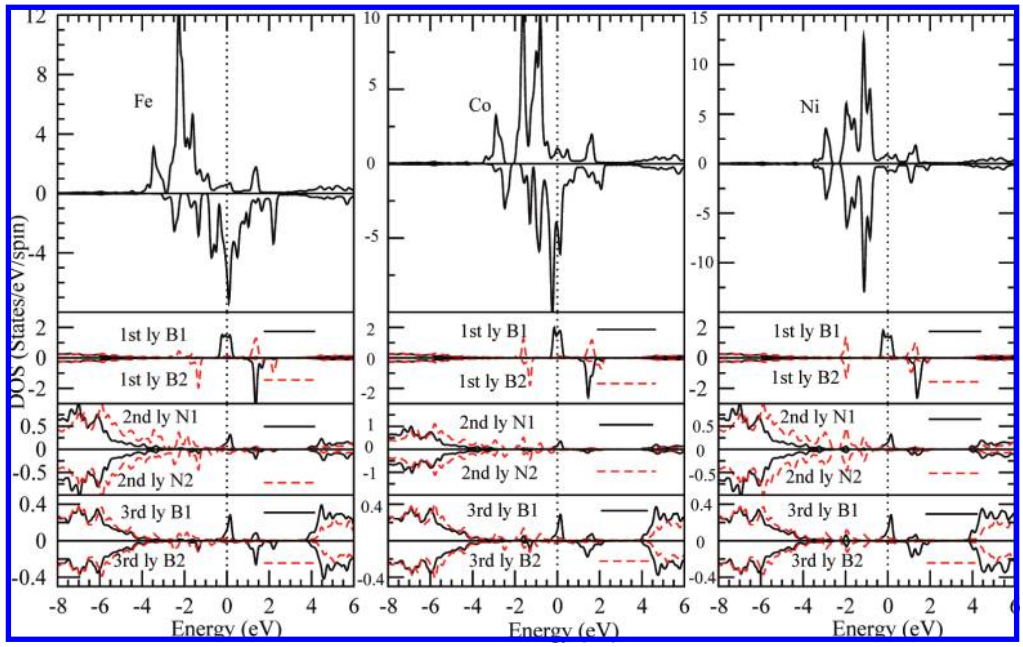

Figure 3. GGA density of states for Fe, Co, and Ni nanowires on the w-BN (0001) surface terminated by B layers. Positive and negative sides are for the up-spin and down-spin parts respectively. The Fermi level is set at zero.

TABLE 7: Calculated Total Energies *E* of the Supercell for Ferromagnetic (FM), Antiferromagnetic (AF), and Nonmagnetic (NM) States Relative to the Ground State for the Fe, Co, and Ni Nanowires on the w-BN (0001) Surface Terminated by N Layers

	Fe	Co	Ni
E_{FM} (meV)	0	0	0
E_{AF} (meV)	129.66	213.14	20.82
E_{NM} (meV)	917.38	855.07	95.53

In the case of the Fe nanowire on the N-terminated w-BN (0001), we find that from −1.0 to −0.2 eV (see Figure 4), the down-spin DOS of Fe and the down-spin DOS of the N1 in the first layer have similar peaks and character. Therefore the Fe down-spin t_{2g} bands hybridize strongly with the N1 down-spin $2p_z$ bands. This hybridization causes the big induced magnetic moments on N1 and N2 of the first layer $-0.437\mu_B$ and $0.12\mu_B$, respectively. It is found that the up-spin Fe d-like orbitals are almost fully filled, and the two down-spin Fe e_g orbitals are nearly empty. The present GGA calculations give spin moments of $3.135\mu_B$/Fe for the Fe nanowires on the N surface of the w-BN (0001), which is nearly the same as the magnetic moment of $3.188\mu_B$/Fe in the isolated Fe chain. High spin polarization is observed in the Fe nanowires on the w-BN (0001) surface terminated by N layers. The present calculations show that the spin moment of Fe in 1D and quasi-1D is much larger than the spin moment value $2.2\mu_B$/Fe of bcc Fe. The spin moment value of Fe in a 2D film is $2.53\mu_B$/Fe (ref 3). These results indicate that in general the magnetic moment of Fe decreases with increasing dimensions.

Now we turn to the Co and Ni nanowires on the N surface of the w-BN (0001). We notice that an unambiguous gap is created around the Fermi Level in the DOS of the up-spin for the top three layers. The center layers (the fifth and sixth layers) demonstrate insulator behavior, and their DOS resemble that of B and N in the bulk BN (see Figure 5). The Fermi level crosses the down-spin orbitals of the Co (Ni) d-like, and N1(in the first layer) pz, and B1 (in the second layer) py and px, and N1 (in the third layer) pz. Thus, the Co and Ni nanwires on the N surface of the w-BN(0001) are half-metallic ferromagnets, and the half-metallic gaps are about 0.35 eV and 0.65 eV for Co and Ni nanowires, respectively. These relatively large gaps make it possible for electric transport through such hybrid structures to be carried out solely by carriers with a single (down) spin state. When the Co and Ni chains are brought into contact with the N surface of w-BN (0001), the hybridization between the Co (Ni) d-like orbitals and N 2p orbitals leads to an appreciable broadening of the Co (Ni) 3d bands. The down-spin orbitals of e_g and t_{2g} distinctly separate from each other compared to that in the free-standing chains and on the B surface of the w-BN (0001). Clearly, there is a strong exchange-splitting in the DOS of the Co (Ni) atom. The spin-splitting are about 2.0 and 1.8 eV for Co and Ni, respectively. Likewise for the spin magnetic moments, these spin-splittings drop dramatically as one goes inward (up−down in Figure 4). The present calculations give the spin moment value of $2.177\mu_B$/Co and $1.113\mu_B$/Ni, which are nearly the same as the case for the free-standing Co (Ni) chain in a vacuum. All TM chains prefer a moment orientation perpendicular to the substrate. Our results for Co nanowires are consistent with experimental values of analogous nanostructures. For example, experiments[7,11,13] have found that the spin moments of Co in a single atom, 1D and 2D are $2.14\mu_B$, $2.14\mu_B$, and $1.74\mu_B$, respectively.

The magnetism of the 3d transitional metal Ni has been extensively studied.[34,35] The calculated spin moments[35] of the hcp Ni nanowires encapsulated in BN nanotubes are $0.67\mu_B$, $0.58\mu_B$, and $0.76\mu_B$ per Ni atom for Ni/BN(8,0), Ni/BN(9,0), and Ni/BN(10,0), respectively. Whereas in Ni chains with light carbon encapsulation at 5 K[22] the magnetic moment decreases to $0.26\mu_B$ per Ni atom. In the present work, the calculated value of a Ni nanowires on the N surface of the w-BN (0001) is $1.113\mu_B$ per atom, which is significantly different from the above theoretical and experimental values for the analogous nanostructures. Hence the dimension and the chemical environment of the ferromagnet have a great effect on the magnetism.

We also calculated the MAE of the ferromagnetic metal atoms. In the following the MAE is defined as the energy difference between the maximum and minimum total energies among E^{100}, E^{010}, and E^{001}, where E^{100}, E^{010}, and E^{001} are the

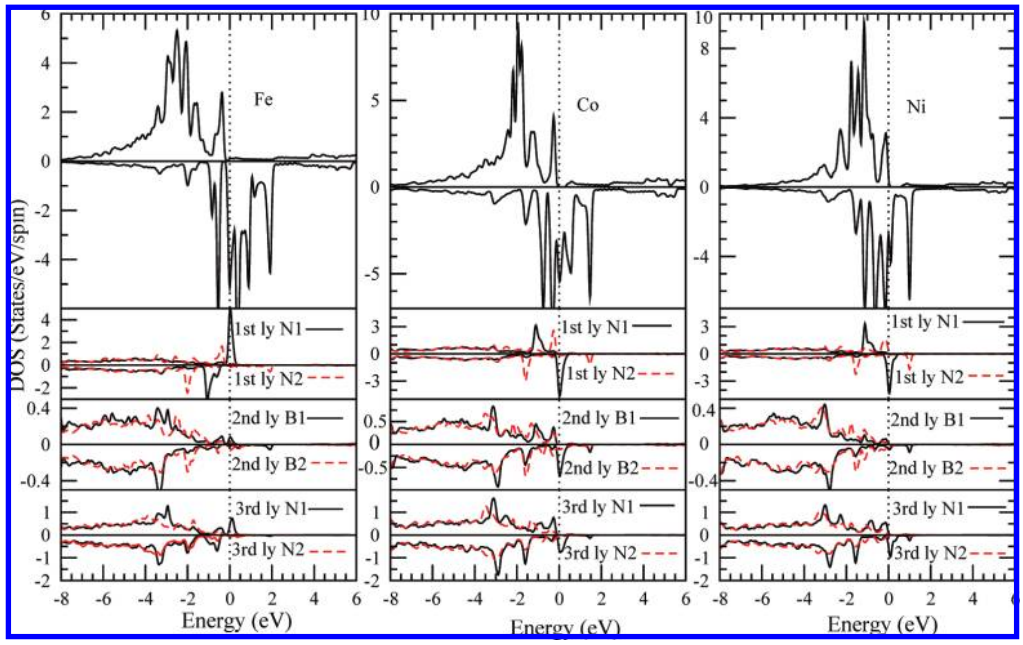

Figure 4. GGA density of states for Fe, Co, and Ni nanowires on the w-BN (0001) surface terminated by N layers. Positive and negative sides are for the up-spin and down-spin parts respectively. The Fermi level is set at zero.

TABLE 8: GGA Calculated Spin Magnetic Moments in μ_B for the Fe, Co, and Ni Nanowires on the w-BN (0001) Surface Terminated by N Layers[a]

	Fe (Co, Ni)	first ly N1	first ly N2	second ly B1	second ly B2	third y N1	third ly N2
Fe	3.135	–0.437	0.12	0.03	0.02	–0.07	0.03
Co	2.177	0.447	0.14	–0.02	–0.00	0.12	0.01
Ni	1.113	0.446	0.17	–0.02	–0.01	0.14	0.01

[a] In the table, the N1 of the first layer denotes the N atom which is the second furtherest away from the nanowire, and the N2 is the nearest neighbor N atom of the nanowires in the first layer. We adopt the same rule to label atoms in other layers. The word layer is abbreviated to ly in this Table and figures.

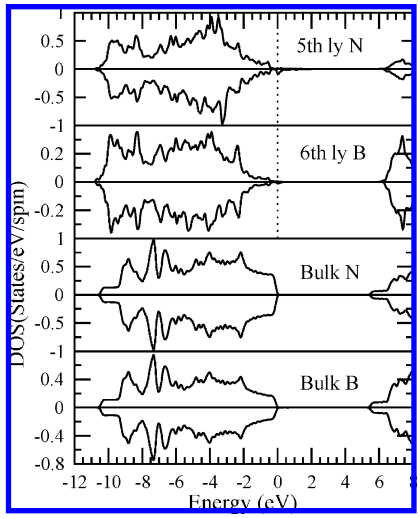

Figure 5. DOSs of the center layers of the substrate and the bulk BN. Positive and negative sides are for the up-spin and down-spin parts respectively. The energy of the highest occupied state for bulk BN is set at zero.

total energies with the magnetization in the [100], [010], and [001] direction, respectively. Table 9 gives the calculated spin and orbital moments with the magnetization in the [001] direction, and the MAE of the magnetic atoms for the Fe, Co, and Ni nanowires on the N surface of the w-BN (0001).

TABLE 9: Spin and Orbital Moments (μ_B) and MAE (meV) per Ferromagnetic Atom Calculated for the Fe, Co, and Ni Nanowires on the w-BN (0001) Surface Terminated by N Layers within the GGA Scheme

	S_z	L_x	L_y	L_z	MAE
Fe	3.135	0.276	−0.282	0.152	0.29
Co	2.177	0.207	−0.121	0.563	0.11
Ni	1.113	0.095	−0.064	0.384	0.12

Table 9 reveals that S and L of the Fe, Co and Ni are noncollinear. Different effects combine in establishing the large MAE of TM chains on the BN surface. (i) The MAE arises mainly from the TM chains which interact weakly with the substrate such as BN surface. (ii) The negligible spin−orbit coupling of the B and N p-states in the substrate will not affect much the MAE of the induced magnetization. (iii) The reduced coordination leads to 3d-electron localization (band narrowing), which augments the spin−orbit energy due to increases in the local DOS near the Fermi level and the spin magnetic moments. This anomalous ferromagnetism was also found in the monoatomic Co nanowires at the Pt (111) surface step edge.[36] Noncollinearity of S and L has been previously predicted for noncollinear spin magnetic structures, but not for a collinear spin ferromagnetic configuration.[37] In all cases, the easy axis of magnetization is along [0001] direction. Free TM atoms possess large S and L according to Hund rules. However, the influence of the insulator substrate(as BN surface) on the TM chains causes a small reduction of S and L. We note that the electron delocalization and crystal field effects compete with the intra-atomic Coulomb interactions, responsible for Hund's rules. The rotation of the spin from the out-of-plane to the in-plane direction will change little the S, where the change in L is also small. Indeed, this strong anisotropy in L paves the way for the strong MAE. However, our theoretical findings demonstrate that S and L have not strongly reduced at surfaces owing to the decreased coordination of TM chains. The orbital moments and the MAE of Fe in bcc and Ni in fcc have been studied theoretically and experimentally,[38] the orbital moments

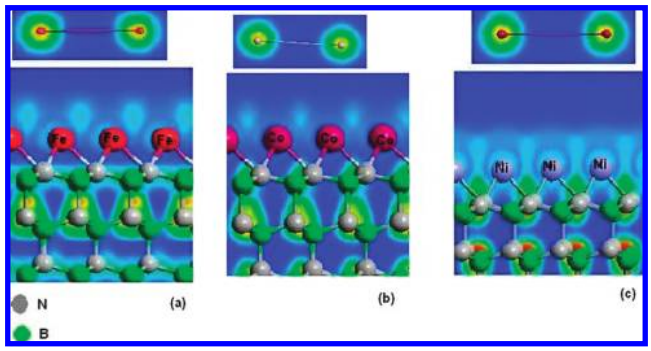

Figure 6. Total charge densities of Fe, Co, and Ni wires adsorbed on w-BN (0001) surface in [0001] direction.

and MAE are 0.08 μ_B/Fe and 0.0014 meV/Fe for bcc Fe, 0.05 μ_B/Ni and 0.0027 meV/Ni for fcc Ni, respectively. The experimental orbital moments value of the Co atom for the hcp bulk and wires on the Pt(997) surface are 0.14 μ_B, 0.68 μ_B, respectively;[13,38] the MAE of Co for a Co chain on the Pt(997) surface, and a biatomic chain and monolayer film on Pt (997) are 2.0 meV, 0.34 meV and 0.13 meV respectively.[13] For Co nanoparticles on the Pt(111) surface, the orbital magnetic moment and MAE decrease strongly with increasing Co coordination, from 1.10 μ_B for the single Co adatom to 0.22 μ_B/Co for the tetramer; and 18.45 meV /Co for the single Co adatom to 0.75 meV/atom for tetramer.[11] The orbital moments and MAE of the Fe, Co and Ni nanowires on the N surface of the w-BN (0001) depend sensitively on the coordination of the ferromagnetic atoms. Our results are in qualitative agreement with the experimental results of the analogous nanostructures. The above results indicate that the large MAE stems from the larger spin−orbit coupling of the ferromagnetic atom and the strong hybridization between the ferromagnetic atoms and atoms of the substrate.

E. Nature of the Adsorption-BN Bond (Ad = Fe, Ni, and Co). To further explore the interaction between the TM (=Fe, Co, and Ni) chains and BN surface, we calculate their corresponding valence charge densities. Figure 6a−c represent the 2D plots of the total valence charge distributions on a plane perpendicular to the surface. We notice that the valence charge density is primarily localized around the Fe, Co, and Ni atoms and extends slightly to the N atoms of the first surface layer (see Figure 6a−c). It is clearly seen that the charge population for Fe, Co, and Ni atoms adsorbed on the surface takes place mostly along [0001] direction. The interaction between the TM chains and surface N atoms can at first be understood just on a simple electrostatic basis. In fact the formation of the Fe−N or Co−N bonding states induces a charge depletion around the top surface layer. The charge population around Fe, Co, and Ni atom in a vacuum direction is a little bit shrunk which indicates weaker TM (Fe, Co, and Ni)-N interaction and a smaller polarization of the bond. Our theoretical Fe−N bond length for 1 × 2 unit cell being 2.491 Å is close to the sum of the Fe (2.35 Å) and N (1.17 Å) covalent radii, moreover they compare well with the minimum bond length of 2.56 Å for the FeN compound. In contrast to Fe, Ni have much weaker bonds to surface N atom due to the higher d-band filling. A charge transfer (approximately 0.19, 0.21, and 0.11e, for Fe, Co, and Ni, respectively) from the surface N p anions to the TM chain d cations occurs. This can be detected by comparing the data for the free-standing chains with those of the TM chains on the N-terminated w-BN (0001). The effect of the interaction is related to the difference of these values. The depletion of N states justifies the charge transfer between the Fe, Co and Ni chains and the substrate. It is also indicated that the reduction of the magnetic moment in TM/BN can be explained in terms of charge transfer from N to TM, and since around the Fermi level mainly the TM d-band states are available. For all TM chains on the N-terminated BN surface, the charge in Fe, Co, and Ni atoms increases compared to the free-standing wires which mainly originated from d states. This indicates a charge flow from N-p states to TM-d orbitals in [0001] direction. In all cases, the contour plot shows a p-d hybridization between the TM chains and the N atoms. It is clear that there are naturally direct hybridizations between TM chains and the substrate. The directional bonds between the TM atoms and surface N atoms can be seen as the charge accumulation white color regions in Figure 6a−c around TM atoms. As expected from electronegativity and atomic numbers, the occupied p states have predominantly N character, while in the d states the TM contribution dominates. In the layer just below the surface, the boron atom loses charge to the nitrogen atom. The charge redistribution both inside the layers and between them is more complicated in boron nitride than in bulk. In the other hand, the absence of Co−Co (Fe−Fe or Ni−Ni) interaction along [0100] direction, neither direct nor mediated by the substrate, strengthens the 1D picture of the assembled structures. It confirms also that the 1 × 2 periodicity along the [0100] direction is sufficient to avoid spurious coupling among parallel Co (Fe or Ni) chains. Nevertheless, to assert that Fe, Co, and Ni wires on BN(0001) surface could be considered as an effective 1D system (as the isolated one), it is necessary to understand the intrinsic coupling with the substrate and characterize the electronic structure of the TM(=Fe, Co, and Ni)/BN interface.

IV. Conclusions

The magnetism of Fe, Co, and Ni nanowires on the w-BN (0001) was studied from first principles calculations using the GGA scheme. It is found that the large MAE of the ferromagnetic metallic atoms is caused by a magnetic Coulomb interaction between the ferromagnetic atoms and nitrogen and boron atoms. In addition, the large spin−orbit coupling of the ferromagnetic metal atoms, and the hybridization between ferromagnetic metal atoms d- and N and B p-like states are crucial. The Fe nanowires on N-terminated w-BN (0001) and monoatomic Co and Fe nanowires on B-terminated w-BN (0001) present large but not complete spin polarization. We have demonstrated that the formation of atomic chains of metals (Co, Ni) is subordinate to the presence of d electrons in the outer shell of the chains, which partially hybridize with p electrons of N states in the BN surface. This leads to p-d hybridization between Fe, Co, or Ni chains and the substrate. The monoatomic Co and Ni nanowires on the N-terminated w-BN (0001) are excellent half-metallic ferromagnets with large half-metallic gaps, which could be promising candidates for spintronics applications. We have also linked the chains-to-substrate interaction with increasing occupation of the d shell from Fe to Co to Ni. Greater occupancy in the d-shell means less coupling. The combination of these two properties justifies the appealing properties of the effective 1D Co (Fe) chains on BN(0001). This theoretical effort is directed toward providing relevant information for future experiments.

Acknowledgment. This work was supported by the National Science Council of Taiwan under Grant No.NSC91-2816-M-002-009-6. One of the authors, A.L., would like to thank L. M. Kettle for reading the manuscript. S.J.L. was supported in part

by the National Natural Science Foundation of China under Grant No. 10447108, the Natural Science Foundation of Hubei province under Grant No. 2005ABA304 and the science and technology research project foundation of the educational department of Hubei province No. D200623001.

Note Added after ASAP Publication. This paper was published on the Web on July 22, 2009, with minor changes made throughout the text. The corrected version was reposted on July 24, 2009.

References and Notes

(1) Himpsel, F. J.; Ortega, J. E.; Mankey, G. J.; Willis, R. F. *Adv. Phys.* **1998**, *47*, 511.
(2) *Ultrathin Magnetic structure*; Bland, J. A. C., Heinrich, B., Eds.; Springer-Verlag: Berlin, 1994.
(3) Elmers, H. J.; Liu, G.; Gradmann, U. *Phys. Rev. Lett.* **1989**, *63*, 566.
(4) Hong, S. C.; Freeman, A. J.; Fu, C. L. *Phys. Rev. B* **1988**, *38*, 12156.
(5) Qian, X.; Hbner, W. *Phys. Rev. B* **1999**, *60*, 16192.
(6) Galanakis, I.; Alouani, M.; Dreysse, H. *Phys. Rev. B* **2000A**, *62*, 3923.
(7) Spisak, D.; Hafner, J. *Phys. Rev. B* **2004**, *70*, 01443.
(8) Gradmann, U.; Waller, G. *Surf. Sci.* **1982**, *116*, 539.
(9) Przybylski, M.; Kaufmann, I.; Gradmann, U. *Phys. Rev. B* **1989**, *40*, 8631.
(10) Elmers, H. J.; Hauschild, J.; Gradmann, U. *Phys. Rev. B* **1996**, *54*, 15224.
(11) Gambardella, P.; Rusponi, S.; Veronese, M.; Dhesi, S. S.; Grazioli, C.; Dallmeyer, A.; Cabria, I.; Zeller, R.; Dederichs, P. H.; Kern, K.; Carbon, C.; Brune, H. *Science* **2003**, *300*, 1130.
(12) Shick, A. B.; Lichtenstein, A. I. *J. Phys.Cond. Matter* **2008**, *20*, 015002.
(13) Gambardella, P. *Nature* **2002**, *416*, 301.
(14) Gambardella, P. *J. Phys.: Condens. Matter* **2003**, *15*, 1.
(15) Mermin, N. D.; Wagner, H. *Phys. Rev. Lett.* **1966**, *17*, 1133.
(16) Hauschild, J.; Elmers, H. J.; Gradmann, U. *Phys. Rev. B* **1998**, *57*, R677.
(17) Schneider, C. M.; Kirschner, J. In Handbook of Surface Science; Horn, K., Scheffler, M., Eds.; Elsevier: Amsterdam, 2000; p 511.
(18) Wolf, S. A.; Awschalom, D. D.; Buhrman, R. A.; Daughton, J. M.; Von Molnar, S.; Roukes, M. L.; Chtchelkanova, A. Y.; Treger, D. M. *Science* **2001**, *294*, 1488. Osborne, I. S. *Science* **2001**, *294*, 1483. Awschalom, D. D.; Kikkawa, J. M. *Phys. Today* **1999**, *52*, 33.
(19) Pickett, E.; Moodera, J. S. *Phys. Today* **2001**, *54*, 39.
(20) de Groot, A.; Mueller, F. M.; van Engen, P. G.; Buschow, K. H. J. *Phys. Rev. Lett.* **1983**, *50*, 2024.
(21) Dong, W.; Chen, L. C.; Palmstrom, C. J.; James, R. D.; Mckernan, S. *Appl. Phys. Lett.* **1999**, *75*, 1443.
(22) Watts, M.; Wirth, S.; von Molnar, S.; Barry, A.; Coey, J. M. D. *Phys. Rev. B* **2000**, *61*, 9621.
(23) Jedema, J.; Filip, A. T.; van Wees, B. *Nature(London)* **2001**, *410*, 345. Soeya, S.; Hayakawa, J.; Takahashi, H.; Ito, K.; Yamamoto, C.; Kida, A.; Asano, H.; Matsui, M. *Appl. Phys. Lett.* **2002**, *80*, 823.
(24) Coey, M. D.; Viret, M.; von Moln, S. **1999**, *48*, 167.
(25) Akimoto, Y.; Moritomo, Nakamura, A.; Furukawa, N. *Phys. Rev. Lett.* **2000**, *85*, 3914. Coey, J. M. D.; Venkatesan, M. *J. Appl. Phys.* **2002**, *91*, 8345. Galanakis, I.; Dederichs, P. H.; Mavropoulos, P. *Phys. Rev. B* **2002**, *66*, 134428.
(26) Berger, L. I. *Semiconductor Materials*; CRC Press: New York, 1997.
(27) Janotti, A.; Wei, S. H.; Singh, D. J. *Phys. Rev. B* **2001**, *64*, 174107.
(28) Perdew, J. P.; Burke, K.; Ernzerhof, M. *Phys. Rev. Lett.* **1996**, *77*, 3865.
(29) Kresse, G.; Hafner, J. *Phys. Rev. B* **1993**, *47*, 17953.
(30) Kresse, G.; Joubert, J. *Phys. Rev. B* **1994**, *49*, 14251.
(31) Kresse, G.; Furthmüller, J. *Phys. Rev. B* **1996**, *54*, 11169.
(32) Janotti, A.; Wei, S.-H.; Singh, D. J. *Phys. Rev. B* **2001**, *64*, 174107.
(33) Elmers, H. J.; Hauschild, J.; Fritzsche, H.; Liu, G.; Gradmann, U.; Köhler, U. *Phys. Rev. Lett.* **1995**, *75*, 2031.
(34) Xiang, H. J.; Yang, J.; Hou, J. G.; Zhu, Q. *New J. Phy.* **2005**, *7*, 39.
(35) Zheng W. Z. et al.,arxiv.org/cond-mat/0510168 (unpublished). "Size-dependent magnetic properties of Nickle nano-chains" (to be published).
(36) Shick, A. B.; Mca, F.; Oppeneer, P. M. *Phys. Rev. B* **2004**, *69*, 212410.
(37) Sandratskii, L. M. *Adv. Phys.* **1998**, *47*, 91.
(38) Trygg, J.; Johansson, B.; Eriksson, O.; Will, J. M. *Phys. Rev. Lett.* **1995**, *75*, 2871.

JP810124K